Primer Length Dependence of Binding of DNA Polymerase I Klenow Fragment to Template−Primer Complexes Containing Site-Specific Bulky Lesions†

Olga Rechkoblit,‡ Shantu Amin,§ and Nicholas E. Geacintov*,‡

Chemistry Department, New York University, New York, New York 10003-5180, and American Health Foundation, Valhalla, New York 10595

Received March 17, 1999; Revised Manuscript Received June 30, 1999

ABSTRACT: The binding of the benzo[*a*]pyrene metabolite *anti*-BPDE (*r*7,*t*8-dihydroxy-*t*9,10-epoxy-7,8,9,10-tetrahydrobenzo[*a*]pyrene) to the N^2 group of 2′-deoxyguanosine residues (dG*) is known to adversely affect the Michaelis−Menten primer extension kinetics catalyzed by DNA Pol I and other polymerases. In this work, the impact of site-specific, *anti*-BPDE-modified DNA template strands on the formation of Pol I (Klenow fragment, KF)/template−primer complexes has been investigated. The 23-mer template strand 5′-d(AAC G*C-$_1$ T$_{-2}$ ACC ATC CGA ATT CGC CC), **I** (dG* = (+)-*trans*- and (−)-*trans*-*anti*-BPDE-N^2-dG), was annealed with primer strands 18, 19, or 20 bases long. Complex formation of these template−primer strands with KF^- (exonuclease-free) at different enzyme concentrations was determined using polyacrylamide gel mobility shift assays in the absence of dNTPs. The lesion dG* causes an increase in the dissociation constants, K_d, of the monomeric, 1:1 KF^-/DNA template−primer complexes by factors of 10−15 when the 3′-end base of the primer strand is positioned either opposite dG*, or opposite dC$_{-1}$ in **I**, and the shapes of the binding isotherms are sigmoidal. The sigmoidal shapes are attributed to the formation of dimeric 2:1 KF^-/DNA template−primer complexes. In contrast, when the 3′-end of the primer strand extends only to dT$_{-2}$ in **I**, the K_d of 1:1 complexes is increased by factors of only 2−3, the shapes of the binding isotherms are hyperbolic and nonsigmoidal and are similar to those observed with the unmodified control, and monomeric KF^-/DNA complexes are dominant. The impact of bulky lesions on polymerase/DNA complex formation in polymerase-catalyzed primer extension reactions needs to be taken into account in interpreting the site-specific Michaelis−Menten kinetics of these reactions.

The influence of the bulky lesions derived from the binding of the mutagen *r*7,*t*8-dihydroxy-*t*9,10-epoxy-7,8,9,10-tetrahydrobenzo[*a*]pyrene (*anti*-BPDE)[1] to the N^2 group of 2′-deoxyguanoisine residues on DNA replication in vitro has been investigated using purified polymerases in vitro (*1*−*3*). Site-specifically modified oligonucleotide templates (*4*) are particularly useful in these kinds of studies. Primer extension kinetics can be determined by measuring the initial reaction rates at different concentrations of 2′-deoxynucleoside 5′-triphosphates (dNTP) under steady-state conditions in order to extract the Michaelis−Menten parameters V_{max} and K_m at specific sites of the modified template strands (see, for example, ref *1*). In the Michaelis−Menten model, one of the important critical initial steps is the formation of *ternary* complexes when the dNTPs bind to the polymerase/template−primer complexes. The concentrations of the *binary* enzyme/template−primer complexes depend on the enzyme and DNA concentrations, as well as on their dissociation constants, K_d. The Michaelis−Menten kinetics are generally determined under conditions of excess DNA concentrations, and variations in K_d due to the bulky lesions are usually neglected. However, bulky adduct-modified bases positioned at or near the single strand−double strand junctions in template−primer complexes may, in principle, have an effect on the dissociation constant K_d, as was recently demonstrated in the case of *N*-acetyl-2-aminofluorene- and *N*-2-aminofluorene-modified DNA (*5*). In this work we investigated the effect of position of the 3′-end of a primer strand relative to the position of a BPDE-modified dG residue in the template strand on the efficiencies of formation of polymerase/template−primer complexes using DNA Pol I Klenow fragment (exonuclease-free, KF^-). The lesions were derived from the binding of the mutagenic enantiomers (+)-(7*R*,8*S*,9*S*,10*R*) and (−)-(7*S*,8*R*,9*R*,10*S*) of *anti*-BPDE to N^2-dG (*trans*-*anti*-[BPDE]-N^2-dG, Scheme 1) to the oligodeoxynucleotide 5′-d(AAC[G*]CTACCATCCGAATTCGCCC). This particular oligonucleotide was selected for study for two reasons: (1) the impact of (+)-*trans*- and (−)-*trans*-*anti*-[BP]-N^2-dG lesion on the alignment of the bases at the single strand−double strand junctions in the same sequence context has been studied earlier by NMR methods (*6*, *7*), and (2) relatively short single-stranded overhangs (3−5 bases long) were selected in order to enhance the impact of the lesions on the polymerase/DNA binding parameters. It has

† This research was supported by NIH Grant CA20851. The benzo[*a*]pyrene diol epoxides were supplied by the National Cancer Institute Carcinogen Reference Standard Repository.

* To whom correspondence should be addressed.

‡ New York University.

§ American Health Foundation.

[1] Abbreviations: BP, benzo[*a*]pyrene; BPDE or *anti*-BPDE, *r*7,*t*8-dihydroxy-*t*9,10-epoxy-7,8,9,10-tetrahydrobenzo[*a*]pyrene; KF^-, Klenow fragment of DNA Pol I (exonuclease-free); dNTP, 2′-deoxynucleotide triphosphate; BSA, bovine serum albumin; DTT, dithiothreitol; EDTA, ethylenediaminetetraacetic acid; HPLC, high-performance liquid chromatography; Tris, tris(hydroxymethyl)aminomethane.

10.1021/bi990614k CCC: $18.00
Published on Web 08/17/1999

Scheme 1: (+)-*trans*-*anti*-BPDE-dG[a]

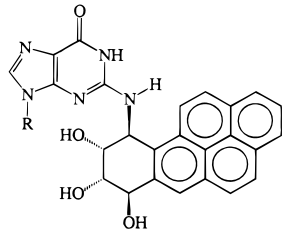

[a] The (−)-*trans* stereoisomeric adduct has opposite stereochemical properties at each chiral atom.

been shown, using different footprinting and other experiments, that 5−8 bases of the single-stranded portion of the template strand (beyond the 3′-end terminus of the primer positioned at the polymerase active site) are in contact with the large cleft of the polymerase domain (*8*−*10*). Therefore, a longer template strand might have obscured the effects of the modified bases positioned at or near the 3′-terminus of the primer.

The *anti*-BPDE diol epoxides are generated metabolically from benzo[*a*]pyrene, a ubiquitous and widely studied environmental pollutant (*11*). Their modes of binding to native DNA is well established (*12*, *13*). The presence of these bulky lesions in site-specifically modified DNA sequences is known to block DNA synthesis and to allow, infrequently, error-prone bypass that can cause mutations in vitro (*3*, *14*, *15*) and in cellular systems (*16*−*19*). Recently, Denissenko et al. (*20*) showed that the distribution of BPDE-dG adducts along exons of the p53 gene in BPDE-treated HeLa cells match the major mutational hot spots of the p53 gene in human lung cancers; these findings suggest that BPDE-modified dG residues are involved in generating mutations which inactivate this tumor suppressor gene.

The values of the Michaelis−Menten parameters measured in the vicinity of single site-specific *anti*-BPDE-N^2-dG lesions in the template strand depend strongly on the site of the dNTP incorporation relative to the site of the lesion (*1*, *21*). In general, the lesions were found to severely inhibit translesional synthesis, and the mutational misincorporation of the incorrect bases depends on the stereochemical characteristics of the lesions (*1*, *21*). The positions of the modified dG residues relative to the single strand−double strand junctions also significantly affect the magnitudes of V_{max} and K_m in a manner that is not well understood.

The DNA repair polymerase Pol I Klenow fragment from *Escherichia coli* (KF) is one of the most extensively studied and characterized DNA synthesizing enzymes. The three-dimensional structures of the binary complex of the Klenow fragment with DNA (*22*) and the polymerase−dNTP complex (*23*), along with extensive kinetic and biochemical studies (reviewed in ref *24*), suggest that this enzyme is a useful model system for studying the effects of DNA adducts on template-directed DNA synthesis. The Klenow fragment lacking 3′,5′ exonuclease activity (KF^-) exhibits a normal level of polymerase activity (*25*, *26*). The mechanism of polymerase-catalyzed DNA synthesis includes several key steps that have been extensively discussed (*26*, reviewed in ref *27*). The focus of this work is on the impact of a (+)- and (−)-*trans*-*anti*-BPDE-N^2-dG lesion on the first step in this complex chain of events, namely the efficiencies of formation of the primary polymerase/template−primer complexes in the absence of dNTPs.

Scheme 2[a]

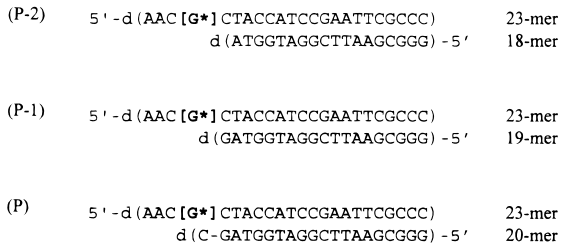

[a] **[dG*]** denotes either an unmodified dG residue or a BPDE-modified dG residue ([dG*] = (+)-*trans*-, or (−)-*trans*-*anti*-BPDE-N^2-dG). The abbreviations (P-2), (P-1), and (P) denote the 23/18, 23/19, and 23/20-mer template−primer DNA complexes, respectively.

The 23-mer template strands with either a (+)-*trans*- or a (−)-*trans*-BPDE-N^2-dG-modified residue [dG*] and the 18-, 19-, 20-mer primer strands that were used as model systems are depicted in Scheme 2. The dissociation constants (K_d) of the different unmodified and BPDE-modified polymerase/DNA complexes were investigated using a gel mobility shift assay. The formation of Klenow fragment/template−primer strand complexes is strongly influenced by the BPDE-N^2-dG lesions, especially when the 3′-end of the primer strand is positioned in the immediate vicinity of the lesion. Evidence is presented that, under these conditions, the polymerase molecules KF^- bind predominantly as dimers to the BPDE-modified template−primer complexes.

MATERIALS AND METHODS

Materials. The oligonucleotides were synthesized using automated methods based on phosphoramidite chemistry and purified by reverse phase HPLC techniques and polyacrylamide gel electrophoresis as described (*28*). HPLC grade acetonitrile, methanol, and distilled water were purchased from Fisher Chemicals. [γ-^{32}P]ATP (specific activity, >5000 Ci/mmol) was obtained from NEN LifeScience Products, Inc. The *exo*$^-$ and *exo*$^+$ Klenow fragments of *E. coli* polymerase I, T4 polynucleotide kinase, and T4 ligase were purchased form Amersham Life Sciences, Inc. The diol epoxides (+)- and (−)-*anti*-BPDE were obtained from The National Cancer Institute Carcinogen Reference Standard Repository.

Synthesis and Modification of Oligonucleotides. The 13-mers, 5′-d(AAC[G*]CTACCATCC) ([dG*] = *anti*-BPDE-modified position), were previously employed in studying the NMR solution conformations of template−primer complexes (*6*, *7*) and were prepared, isolated, and purified according to previously developed procedures (*29*, *30*). The carcinogen-containing 23-mers were constructed by ligating the BPDE-modified 13-mers with the 10-mer 5′-d(GAATTCGCCC) phosphorylated at the 5′-end using the 20-mer template 5′-d(CGAATTCGGATGGTAGCGTT) and T4 ligase. The reaction mixtures were kept at 4 °C for 13 h, and the 23-mer oligonucleotides were separated by gel electrophoresis on 20% polyacrylamide gel in the presence of 7 M urea.

Measurement of the Klenow Fragment Binding Affinity. The dissociation constants, K_d, for all Klenow fragment/DNA complexes was determined using a gel mobility shift assay. The primer strands were labeled at the 5′-end using T4 polynucleotide kinase and [γ-^{32}P]ATP and then purified using denaturing 20% polyacrylamide gel electrophoresis containing 7 M urea. The unmodified and BPDE-dG-modified DNA

template−primer complexes were prepared by annealing the template and primer strands (3-fold excess of the template strand) and heating the solution to 90 °C, followed by slow cooling to room temperature. For a typical experiment, 3 μL of the Klenow fragment solution were added to 7 μL of the DNA template−primer solution. The template−primer DNA complex concentrations used in the experiments were 3 nM. Solutions containing the polymerase and the DNA complexes were incubated for 15 min at 4 °C in 50 mM Tris-HCl (pH 7.5), 10 mM $MgCl_2$, 1 mM DTT, 10% (v/v) glycerol, and loaded into a 7% native polyacrylamide gel (the running buffer was 25 mM Tris borate, 2 mM $MgCl_2$, 0.5 mM EDTA). The samples were electrophoresed at 4.5 V/cm; after 5 min the voltage was reduced to 3.4 V/cm, and electrophoresis was carried out for 4 h at 4 °C. The gel was subsequently dried, exposed to an imaging plate, and analyzed quantitatively using a BioRad GS-525 PhosphorImager scanner.

Comparison of the Electrophoretic Mobilities of Klenow Fragment/DNA Complexes to Those of Bovine Serum Albumin Molecular Weight Standards. Fourteen milligrams of a BSA molecular weight standard (Sigma) was dissolved in 15 μL of 25 mM NaCl−0.5 mM Na_2PO_4 (pH 7), 25 mM Tris borate, 2 mM $MgCl_2$, 0.5 mM EDTA, 15% (v/v) glycerol buffer. The KF/DNA complexes and free DNA template−primer complexes (same conditions as those described above) were loaded onto a nondenaturating gel and electrophoresed as described. The BSA bands were visualized by staining with Coomassie Brilliant Blue R, as described in Sigma Technical Bulletin No. MKR-137, and the ratio of migration distances of the BSA monomer and dimer bands were measured. The gels were then dried, autoradiographed, and the ratio of the migration distances of the two KF/DNA complex bands were also determined and compared to the analogous ratio obtained from the two BSA bands.

Competition between (+)-trans-BPDE-(P-1) and Unmodified (P-1) Complexes for Binding with KF$^-$. Eight samples of template−primer DNA complexes were prepared by mixing the same volume of the (+)-*trans*-BPDE-23-mer/^{32}P 5′-end-labeled 19-mer template−primer complex solution and different amounts of the unmodified 23-mer template. The ratio of the modified to unmodified template strands was varied in the interval from 1:0 to 1:24. The concentration of the template strand was always in excess (10%) as compared to the primer strand, and the overall concentration of the primer strand was kept constant (3 nM). The resulting solutions were heated to 90 °C, followed by slow cooling to room temperature. The KF/DNA complexes were prepared as described above. The concentrations of KF$^-$ were 500 nM in all of the samples.

KF$^-$ Protein Dimer Formation in the Absence of DNA by Gel Electrophoresis. Solutions with different concentrations of KF$^-$ (in the range 200−1700 nM) were prepared by sequential dilution with a buffer solution (50 mM Tris-HCl, pH 7.5, 10 mM $MgCl_2$, 1 mM DTT, 10% glycerol (v/v), 0.002% bromophenol blue). Aliquots of these solutions containing about 400 ng of KF$^-$ were loaded onto native 10% PAGE Tris-HCl gel with a 4% stacking gel (Ready gel, BioRad) and electrophoresed at 150 V for 1 h. The protein bands were detected using a commercially available silver staining procedure (Amersham Pharmacia Biotech silver kit).

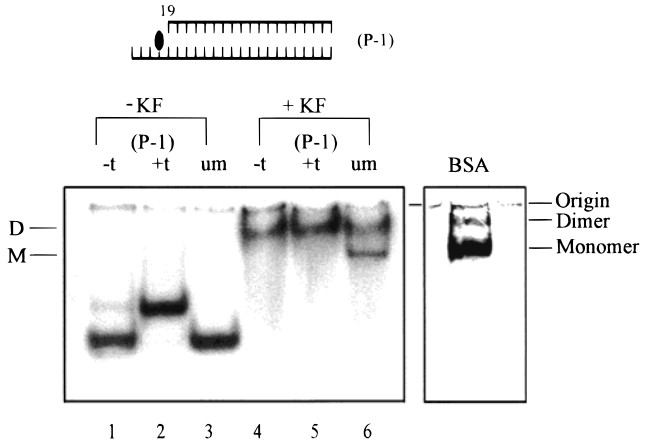

FIGURE 1: Typical gel electrophoretic mobility shift assays using unmodified (um) and BPDE-modified (P-1) template−primer complexes (3 nM) in the absence of KF$^-$ (lanes 1−3) and in the presence of KF$^-$ (344 nM) (lanes 4−5). The designations +*t* and −*t* refer to template complexes with (+)-*trans*- and (−)-*trans*-*anti*-BPDE-*N*^{2}-dG lesions. The two KF$^-$/template−primer complexes labeled M and D exhibit approximately the same mobilities as the monomeric and dimeric BSA complexes, respectively (right-hand panel).

RESULTS

Complex formation between the polymerase KF$^-$ and different template−primer complexes in the absence of dNTPs was studied using the unmodified and (+)-*trans*- and (−)-*trans*-BPDE-modified template−primer complexes (P-2), (P-1), and (P) (Scheme 2).

Stabilities of Template−Primer Complexes. It was important to first verify that stable DNA template−primer complexes are formed under the conditions of the gel running experiments. The gel electrophoresis characteristics of ^{32}P-end-labeled 19-mer primer strands (about 3 nM) in the presence of a 3-fold excess of the 23-mer template strands are depicted in Figure 1 (lanes 1−3). In the presence of the polymerase (344 nm KF$^-$, lanes 4−6), only the lower mobility bands due to the polymerase/DNA complexes are evident. This indicates that neither single- nor double-stranded, polymerase-free DNA molecules are present under these conditions.

Quantitative analysis of these autoradiographs in the absence of KF$^-$ (lanes 1−3) indicates that at least 95% of the two strands migrate as one single complex (the (P-1) complex; the mobility of the single-stranded 19-mer primer strand is faster than the mobilities of the template−primer complexes (data not shown). The mobility of the template−primer complex with the (+)-*trans* lesion is markedly slower than the mobility of the unmodified or the (−)-*trans*-modified (P-1) complexes. Analogous differences in the electrophoretic mobilities of duplexes with (+)- and (−)- *trans*-BPDE-*N*^{2}-dG adducts have been observed in other sequence contexts in double-stranded DNA (*31*−*34*). However, when the adducted site dG* is one base removed from the single strand−double strand junction as in the (P-2) complexes, the electrophoretic mobilities of the (+)-*trans*-modified template−primer complexes are nearly identical to those of the (−)-*trans*-modified and unmodified (P-2) complexes (data not shown).

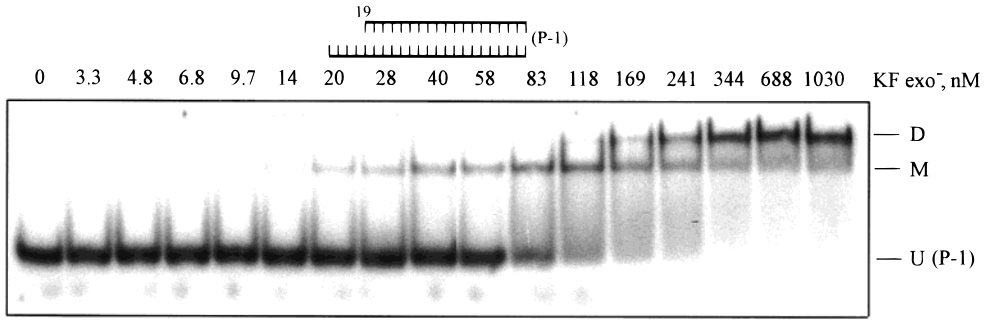

FIGURE 2: Dependence of complex formation between the unmodified (P-1) template−primer complexes (3 nM) as a function of KF^- complexes in the range of 0−1030 nM. D, 2:1 KF^-/DNA complexes; M, 1:1 KF^-/DNA complexes; U (P-1), free unmodified (P-1) template−primer complexes.

KF^-/Unmodified Template−Primer Complex Formation. A gel mobility shift assay was used to determine the equilibrium dissociation constant, K_d, of the complexes. We first examined the affinity of binding of the unmodified template−primer complexes (P-2), (P-1), and (P).

The results of typical gel mobility shift experiments performed at constant concentrations of the unmodified (P-1) template−primer complexes (3 nM) at different enzyme concentrations are shown in Figure 2. As the enzyme concentration is increased, the intensity of the free template−primer complexes (labeled U (P-1)) diminish. At the lower KF^- concentrations a single, lower-mobility band is visible (labeled M), while at the higher concentrations a second, even slower-mobility band develops (labeled D). At the highest enzyme concentrations, two types of low-mobility enzyme/DNA complexes are observed (bands M and D, Figure 2).

A reasonable assumption is that the two bands correspond to monomer and dimer enzyme/template−primer complexes. This hypothesis is supported by the earlier work of Astatke et al. (*35*), who studied complex formation between KF and template−primer DNA complexes containing hairpins. They observed two different enzyme/DNA complexes and assumed that the faster running complex consisted of one molecule of the polymerase bound to the template−primer complex, while the slower migrating complex contained one or more additional enzyme molecules in the enzyme/DNA complex.

The relative molecular weights of the complexes in bands D and M could not be determined by the usual Ferguson method (*36*) because of the partial dissociation of the complexes during the course of the gel running experiments. Other, routine methods for determining molecular weights of the complexes, such as gel filtration or dialysis, require impractical large amounts of the enzyme. To evaluate the complex stoichiometry in the slowest migrating band D, the electrophoretic mobilities of the KF^- complexes (molecular weight 72 kDa) were compared with those of the bovine serum albumin (BSA) monomer and dimers (66 and 132 kDa), respectively. The Klenow fragment and monomer BSA proteins have similar molecular weights. If we assume that the mobilities of the two types of proteins follow the Ferguson relationship (*36*) and that the mobility of each is proportional to $-\log(M)$, where M is the molecular weight, then the differences in mobilities between the pairs of bands due to monomers and dimers should be similar in value at a given gel concentration. The mobilities of the BSA monomer and dimer BSA bands (Figure 1, right-hand panel) are

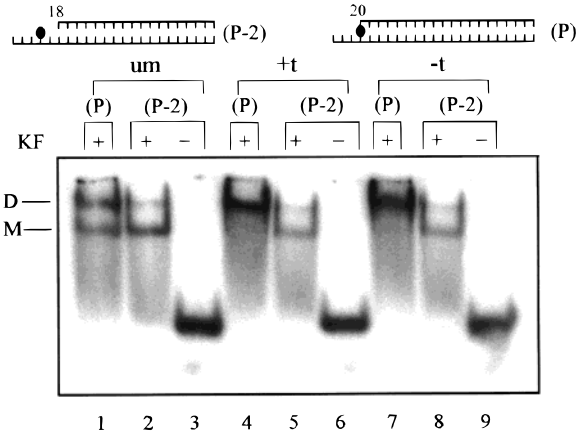

FIGURE 3: Gel electrophoretic mobility shift assays of unmodified (um) and BPDE-modified (+*t* and −*t*) (P) and (P-2) template−primer complexes in the presence of 344 nM KF^- (lanes 1, 2, 4, 5, 7, and 8) and in the absence of KF^- (lanes 3, 6, and 9). D, 2:1 KF^-/DNA complexes; M, 1:1 KF^-/DNA complexes; Um(P-2), free unmodified (P-2) template−primer complexes.

compared to the mobilities of the bands M and D in lanes 4−5 of Figure 1 (left-hand panel). The BSA bands were visualized by staining the gels with Coomassie Brilliant Blue R. The ratio of distances of migration of the BSA monomer and dimer are very close to the distances of migration of the faster (M) and the slower (D) migrating unmodified, or (+)-*trans* and (−)-*trans*-modified, (P-1)/KF^- complexes. These results indicate that the slowest migrating band, D, is due to a complex that contains two polymerase molecules, while M is a complex that contains a single polymerase molecule. While the results shown in the right-hand panel in Figure 1 were obtained in a 10% polyacrylamide gel, identical results were also obtained in a 7% gel, where polymerase dimer formation also occurs only when the KF^- concentration is >1000 nM (data not shown).

The KF^-/BPDE-Modified DNA Template−Primer Complexes. The formation of polymerase/BPDE-modified template−primer complexes can be compared by viewing lanes 4 and 7 (P) and lanes 5 and 8 (P-2) in Figure 3 and lanes 4 and 5 (P-1) in Figure 1. Interestingly, only the putative dimeric KF^- complexes are apparent in the case of the (P) and the (P-1) complexes, while monomeric enzyme complexes are dominant in the case of the (P-2) template−primer complexes. In contrast, in the case of the unmodified template−primer complexes both monomeric and dimeric bands appear in an enzyme concentration-dependent manner (Figure 2). For example, at an enzyme concentration of 344

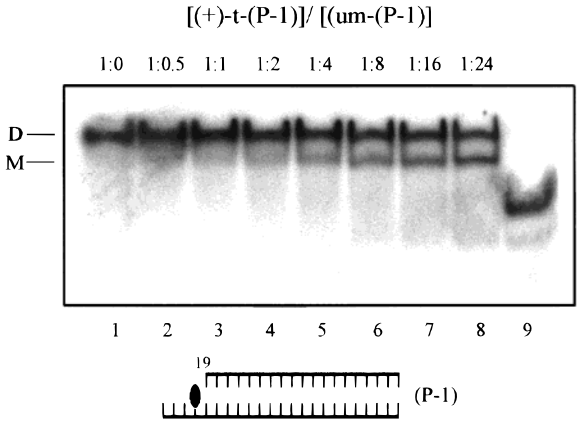

FIGURE 4: Competition between (+)-*trans*-BPDE-modified (P-1) and unmodified (P-1) template−primer complexes for binding with KF^-. The ratio of (+)-*trans*-BPDE modified (P-1) to unmodified (P-1) DNA increases from 1:0 to 1:24 lanes 1−8. The KF^- concentration is constant (500 nM), and the template− primer concentration is 3 nM. Lane 9: (+)-*trans*-BPDE-modified (P-1) without the enzyme. D, 2:1 KF^-/DNA complexes; Mm 1:1 KF^-/DNA complexes; U(P-1), free unmodified (P-1) template−primer complexes.

nM, both the monomer and dimer complexes are evident in the case of the unmodified (P-1) complexes, while only the dimer band is visible in the BPDE-modified complexes under the same conditions (Figure 1, lanes 4−6). Analogous effects are observed in the case of the KF^-/(P) complexes, when the terminal base on the 3′-end of the primer strand is positioned opposite the BPDE-modified dG residue (Figure 3, lanes 4, 7). When the 3′-terminus of the primer strand is one base removed from the lesion site on the 3′-side of the template strand as in the (P-2) complexes, the major KF^-/BPDE-modified (P-2) complexes comigrate with analogous monomeric KF^-/unmodified (P-2) complexes (Figure 3, lanes 2, 5, and 8). However, just as in the case of the unmodified template−primer complexes, lane 2), a dimeric complex is also detectable in the case of the BPDE-modified (P-2) complexes (faint upper bands in lanes 5 and 8, Figure 3).

In summary, the effects of the BPDE-N^2-dG lesions on complex formation with KF^- manifest themselves only if the 3′-terminal base on the primer strand is adjacent to or is opposite to the BPDE-modified dG residue.

Competition Binding Experiments. In the range of KF^- concentrations of 169−344 nM and a 3 nM unmodified (P-1) template−primer complex concentration, the complexes formed contain both one and two enzyme molecules (Figure 2). In contrast, the complex contains primarily two enzyme molecules per (+)-*trans-anti*-BPDE-modified (P-1) template−primer complex (Figure 4, lane 1). In the binding competition experiments depicted in lanes 2−9 of this figure, the overall template−primer concentration was maintained at a constant value of 3 nM, and only the primer strand was ^{32}P-end-labeled. As the ratio of (BPDE-modified)/(unmodified) template strands is increased while the total template strand concentration is held constant, a monomeric enzyme/DNA complex is formed as indicated by the appearance of a higher-mobility band in lanes 5−8. These experiments indicate that the (+)-*trans*-BPDE-modified template strands can be displaced by an unmodified template strand of the same length and base sequence in these KF^-/(+)-*trans*-modified (P-1) complexes. Therefore, at the same KF^- and DNA complex concentrations, the Klenow fragment binds predominantly as a dimer to the BPDE-modified (P-1) complex (lane 1), and as a monomer and dimer to the unmodified (P-1) complex (lane 8).

Estimation of the Dissociation Constants, K_d. The gel mobility shift assays indicate that, during the gel running experiment, some of the KF/template−primer complexes dissociate (∼10−15%). This effect accounts for the radioactivity visible between the lower, higher-mobility, free template−primer complexes and the upper bands due to the enzyme/template−primer complexes. This smeared portion of the gel corresponds to ^{32}P-end-labeled oligonucleotides that dissociate from the enzyme during the gel running experiment; this dissociation was taken into account in calculating the fractions of bound DNA molecules at equilibrium, i.e., when the solutions containing the complexes were loaded onto the gels and before the gel electrophoresis was initiated. This approach is appropriate because only the DNA that was initially bound to the enzyme can gives rise to material with apparently slower mobilities than the initially free DNA.

Since both the monomeric and dimeric enzyme/DNA complexes were subject to dissociation during the gel running experiments, it was generally not possible to evaluate the concentrations of these two complexes separately. The fractions of the total KF^-/DNA complexes are plotted as a function of the KF^- concentration on a semilogarithmic scale in Figure 5. The smaller insets in Figure 5A,C show the same data points on a linear enzyme concentration scale in order to stress the differences in the shapes of the binding curves. In the case of all three types of (P-2) template−primer complexes and the unmodified (P) complex (Um-(P)), the shapes of the binding curves resemble normal binding isotherms. However, in the case of the BPDE-modified (P-1) and (P) template−primer complexes, the binding curves are sigmoidal in shape, as illustrated in the case of the (+)-*trans*-modified (P) complex in the inset in Figure 5C.

The binding curves can be described in terms of the following simple two-step binding model:

$$[\mathrm{E}\cdots\mathrm{DNA}] \xrightarrow{K_{d1}} \mathrm{E} + \mathrm{DNA} \qquad (1)$$

$$[\mathrm{E}\cdots\mathrm{DNA}\cdots\mathrm{E}] \xrightarrow{K_{d2}} \mathrm{E} + [\mathrm{E}\cdots\mathrm{DNA}] \qquad (2)$$

where K_{d1} and K_{d2} are the dissociation constants of the monomeric (E···DNA) and the dimeric (E···DNA···E) enzyme/DNA complexes, respectively. An alternative model in which two enzyme molecules first form a dimer and then bind to the DNA was also considered. However, this model was discarded because, in the absence of DNA, enzyme dimer complexes were not observed (using a silver staining protein detection kit) as long as the KF^- concentration was kept below 1000 nM (see the Supporting Information section). Another model in which the polymerase and DNA first form 1:1 complexes, followed by the dimerization of these 1:1 complexes, was also considered. However, this model is not appropriate either. It can be shown that the binding isotherms would be normal hyperbolic in that case, rather than sigmoidal, as observed experimentally (Figure 5).

Using eqs 1 and 2, the following equations for the monomeric ([DE]) and dimeric ([DE_2]) complexes can be

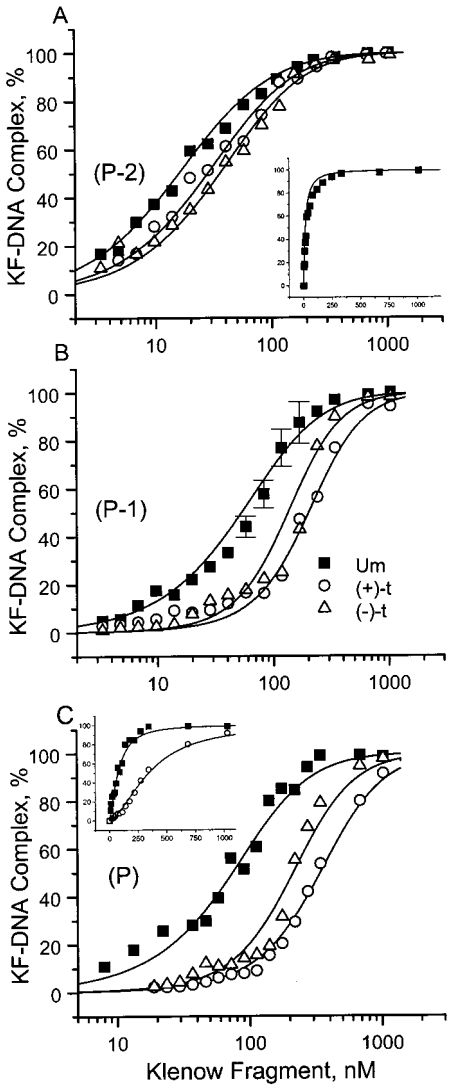

FIGURE 5: Semilogarithmic plots of the fractions of unmodified (Um) and BPDE-modified (P-2), (P-1), and (P) template−primer complexes with (+)-*trans*- (+*t*), and (−)-*trans*- (−*t*) BPDE-N^2-dG lesions as a function of KF^- concentration. Examples of the same data plotted on linear enzyme concentration scales are shown in panels A and C. The experimental data points are represented by black squares (Um), open circles (+*t*), and open triangles (−*t*). The solid lines represent the best fits to the experimental data of calculations of complex concentrations based on the monomer/dimer KF^- binding model (eqs 1 and 2), and the quadratic equation based on eqs 3, 4, and 5 (see Supporting Information), and the values of K_{d1} and K_{d2} (Table 1).

derived:

$$[DE] = (D_0E_0 - 2D_0[Y] - E_0[Y] + 2[Y]^2)/(K_{d1} - D_0 + [Y]) \quad (3)$$

$$[DE_2] = (K_{d2} + E_0 - ((K_{d2} + E_0)^2 - 4(E_0[Y] - [Y]^2))^{0.5})/2 \quad (4)$$

where D_0 denotes the total DNA template−primer concentration (which was 3 nM), and E_0 the overall enzyme concentration. We define the total concentrations of enzyme/DNA complexes, Y, as

$$[Y] = [DE] + [DE_2] \quad (5)$$

Table 1: Complex Formation of the Klenow Fragment (*exo*$^-$) of DNA Pol I and Template−Primer DNA

Monomer complex: $[E\cdots DNA] \overset{K_{d1}}{\rightleftharpoons} E + DNA$

Dimer complex: $[E\cdots DNA\cdots E] \overset{K_{d2}}{\rightleftharpoons} E + [E\cdots DNA]$

DNA template−primer complex	binding curve type	dissociation constants,[a] nM	
		K_{d1}	K_{d2}
unmodified-(P-2)	normal	15 ± 3	200 ± 50
unmodified-(P-1)	normal	65 ± 5	200 ± 50
unmodified-(P)	normal	125 ± 10	100 ± 20
(+)-*trans*-BPDE-(P-2)	normal	30 ± 5	200 ± 50
(+)-*trans*-BPDE-(P-1)	sigmoidal	1000 ± 200	20 ± 5
(+)-*trans*-BPDE-(P)	sigmoidal	1500 ± 250	100 ± 20
(−)-*trans*-BPDE-(P-2)	normal	40 ± 5	200 ± 50
(−)-*trans*-BPDE-(P-1)	sigmoidal	1000 ± 200	50 ± 15
(−)-*trans*-BPDE-(P)	sigmoidal	1500 ± 250	40 ± 15

[a] K_{d1} of the complex formed by Klenow Fragment *exo*$^+$ and unmodified (P-1) template−19-mer primer complex is 70 nM.

and define the monomer and dimer complex dissociation constants K_{d1} and K_{d2} as follows:

$$K_{d1} = [D][E]/[DE] \qquad K_{d2} = [DE][E]/[DE_2] \quad (6)$$

The eqs 3, 4, and 5 can be combined and solved by employing numerical methods using K_{d1} and K_{d2} as adjustable parameters. The details are described in the Supporting Information section. The values of K_{d1} and K_{d2} thus obtained for the different template−primer complexes are summarized in Table 1. The fourth-order equation derived from eqs 4 and 5 was solved for the single root Y that satisfies the condition $0 \le Y \le D_0$ (= 3 nM) using the K_{d1} and K_{d2} values in Table 1. The binding isotherms thus calculated are represented by the smooth lines in Figure 5A−C.

The Dissociation Constants, K_{d1} and K_{d2}. A normal hyperbolic binding isotherm (solid lines, Figure 5) results from KF^- binding to unmodified (P-2), (P-1), and (P) and to BPDE-modified-(P-2) template−primer complexes, when $K_{d1} \le K_{d2}$. Examples of such hyperbolic curves plotted on a linear enzyme concentration scale are shown in the insets to Figure 5A,C. The calculated binding isotherms, however, are sigmoidal when $K_{d1} \gg K_{d2}$; an example is shown in the inset to Figure 5C.

The contributions of the monomeric and dimeric complexes to the overall binding isotherm can be estimated using eqs 3 and 4, and the values of the dissociation constants given in Table 1. Examples are depicted in Figure 6. In the case of the unmodified (P-2) complex it was possible to experimentally measure the relative concentrations of monomeric 1:1 and dimeric 2:1 KF^-/DNA complexes (open diamonds and inverted open triangles, respectively, in Figure 6A). Because of the tendency of the complexes to dissociate, it was not feasible to measure the concentrations of the 1:1 and 2:1 complexes at all values of enzyme concentrations. The limited experimental values of the concentrations of the two types of complexes are in good agreement with the values calculated from eqs 3 and 4 and the K_{d1} and K_{d2} values in Table 1 (dashed line and dash−dot line, respectively, in Figure 6A).

For the BPDE-modified (P) and (P-1) template−primer complexes, the values of K_{d1} are in the range of 1000−1500 nM, while K_{d2} is 30−100 nM. Thus, the dimeric complexes are some 2 orders of magnitude more stable than the

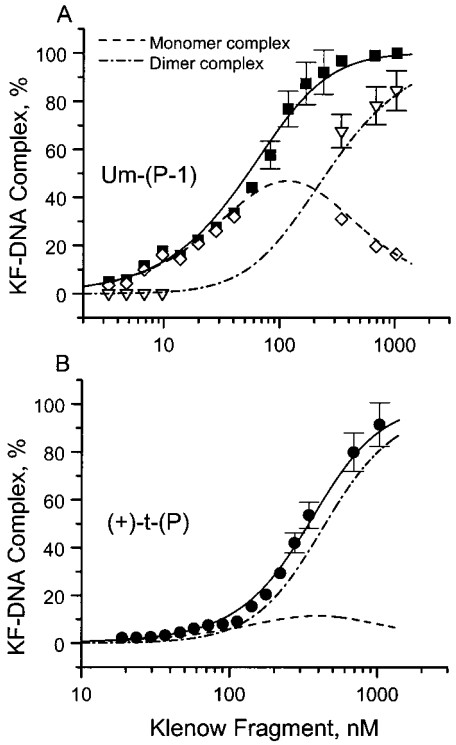

FIGURE 6: Examples of calculations of the concentrations of monomeric 1:1 (dashed lines) and dimeric 2:1 (dash-dot line) KF^-/(P-2) (panel A) and (P) (panel B) template−primer complexes. The (P-1) complex in panel A is unmodified (Um), while the (P) complex bears a (+)-*trans*-*anti*-BPDE-N^2-dG lesion. The calculations of the concentrations of 1:1 complexes ([DE]) and 2:1 complexes ([DE_2]) were calculated using eqs 3 and 4, the appropriate values of K_{d1} and K_{d2} listed in Table 1, and the solution of the quadratic equation based on eqs 3−5 (see Supporting Information). In panel A, the black squares are experimental data points for the total complex concentration, while the open diamonds and open inverted triangles represent experimental data points for the concentrations of 1:1 and 2:1 KF^-/DNA complexes. In panel B, the closed circles represent experimental data points for the overall complex concentrations. The smooth lines fitting the black squares and black circles in panels A and B are the calculated total complex concentrations taken from Figure 5.

monomeric complexes, and their formation is therefore favored in BPDE-modified (P-1) and (P) complexes. When the ss/ds junction is positioned two bases from the lesion site as in (P-2), complex formation with KF^- is similar, both qualitatively and quantitatively, to the case of the unmodified (P-2) template−primer complex. The (+)-*trans* and (−)-*trans*-BPDE-dG residues affect the formation of KF^- complexes to the same extent, even though the conformational characteristics appear to be quite different, at least in the case of (P-1) template−primer complexes (*6*). The presence of the BPDE lesions in the (P) and (P-1) complexes strongly inhibit the formation of the monomeric enzyme complexes, but the formation of dimeric complexes is favored ($K_{d2} \ll K_{d1}$); in contrast, in the case of the unmodified (P) and (P-1) complexes, the K_{d2} are similar or somewhat larger than the K_{d1} values (Table 1), and monomeric complexes are favored.

Complex Formation with KF exo$^+$. The question arises whether the characteristics of the exonuclease domain are somehow related to our observations. The K_d of the analogous complexes with KF *exo*$^+$ (P-1)-template−primer DNA were therefore also determined. As might be expected from the crystal structure of KF *exo*$^+$ (*27*), the modification in the exonuclease site does not significantly affect the stability of the complexes (K_{d1} = 70 nM, data not shown). This value is similar to the one measured with KF *exo*$^-$ (K_{d1} = 65 nM, Table 1).

DISCUSSION

Binding of KF$^-$ *to DNA Template−Primer Complexes*. Footprinting experiments indicate that KF covers 19 and 12 nucleotides on the template and primer strands, respectively (*8*). Other experiments indicate that templates 19−20 nucleotides (*9*) and primers 12 nucleotides in length (*10*) are sufficient to form stable polymerase/DNA complexes. Therefore, the BPDE-modified template strands 23 nucleotides long and the primer strands at least 18 bases long used in our experiments are of sufficient length for measuring the binding of these complexes with KF^-.

Gel mobility shift assays are known to give reliable estimates of the values of K_d characterizing complex formation between the Klenow fragment of DNA polymerase I and DNA molecules with single strand−double strand junctions (*35*). Our K_{d1} values of the unmodified monomeric template−primer complexes are in the range of 15−125 nM (Table 1) and are consistent with other measured K_d values (0.3−200 nM, *24*, *27*, *35*, *37*, *38*). However, our K_{d1} values are higher than those obtained by stopped flow methods (4.5−5 nM) (*37*) and by footprinting and gel retardation techniques (0.3 nM) (*35*) determined for other sequences of similar lengths, but they are much lower than K_d values observed with poly (dA)·oligo(dT) (*38*). The association and the dissociation rate of DNA from KF, as well as the K_d values of the complexes, can also depend on the DNA base sequence and may vary by more than a factor of 10 (*37*).

The stabilities of the KF^-/DNA complexes in the case of the unmodified (P-2) template−primer complex are higher (K_{d1} = 15 nM) than in the case of the (P-1) (K_{d1} = 65 nM) and the (P) template−primer complexes (K_{d1} = 125 nM). The observed reduction of the stabilities of the KF^-/unmodified DNA complexes as a function of increasing primer strand length is most likely related to the effect of the shortened single strand overhang. Joyce et al. (*8*) showed that the strength of the enzyme/DNA interactions decreases by 2 orders of magnitude when the length of the single-stranded region in the template−primer complex is varied from a 4-nucleotide overhang to a blunt-ended duplex. Similar effects were observed by Kuchta et al. (*37*) for 20/17-mer and 19/17-mer template−primer DNA complexes. However, the focus of this study was on comparisons of K_{d1} values with and without the bulky BPDE residues for otherwise identical primer/template complexes, rather than on the magnitudes of the dissociation constants. Since the full 7−9 nucleotide-polymerase contacts (*8*) between the single-stranded template overhang and polymerases would enhances the stabilities of the polymerase/template−primer complexes (*9*, *37*), we selected rather short template overhangs of 3−5 nucleotides long for study in order to enhance the impact of the BPDE residues on the dissociation constants K_{d1}.

Using a 68-mer hairpin oligonucleotide, the existence of complexes with one and two (or possibly more than two) polymerase molecules per DNA molecule was inferred from

gel mobility shift assays by Astatke et al. (*35*). The concentration of a lower-mobility complex was found to increase with increasing KF concentration, and was tentatively identified as a complex consisting of two polymerase molecules. Similar behavior is observed in our experiments with the unmodified template−primer complexes (Figure 2); however, with some of the BPDE-modified complexes, only the lower-mobility presumably polymerase dimer/DNA complexes are observed in a manner which depends on the positions of the BPDE-modified deoxyguanosine residues relative to the 3′-terminus of the primer strand.

Primer Length Dependence of K_d and Conformational Characteristics of Lesions. In the (P-2) complex, when the BPDE-modified dG residue is positioned two nucleotides away from the 3′-terminus of the primer, the bulky adduct exerts a relatively minor effect on the binding of the polymerase molecules to the template−primer DNA complex. The K_{d1} values are 30−40 nM and are only somewhat larger than the values determined for the unmodified (P-2) DNA complex (Table 1). Furthermore, the shapes of the binding isotherms are similar in the case of the unmodified and the BPDE-modified (P-2) template−primer complexes (Figure 5A) and are consistent with a predominant binding of a single polymerase molecule to the template−primer DNA complexes. In a recent study of the binding of DNA Pol I (Klenow fragment) with 28-mer templates and primers 20−22 nucleotides in size, containing single *N*-acetyl-2-aminofluorene (AAF)-C8-dG or N-2-aminofluorene (AF)-C8-dG lesions, it was shown that the length of the primer strands had no significant effect on complex formation. Furthermore, AAF lesions *increased* the stability of the polymerase/DNA adduct (*5*), while no change in the stability of the complexes was observed with AF adducts positioned at or near the polymerase active site. There are significant differences not only in the conformational characteristics of AAF- and AF-C8-dG lesions on one hand (*39*) and the *anti*-[BP]-N^2-dG lesions (*40*) on the other, but also in the design of the experiment and DNA sequences used in our experiments and those of Dzantiev and Romano (*5*). Nevertheless, these results suggest that the modes of interactions between the carcinogen residues and the enzyme may depend significantly on the structure of the carcinogen and their conformations at or near the polymerase active sites.

The mode of binding of KF^- to BPDE-modified templates with primers of different lengths depends remarkably on the proximity of the 3′-end of the primer strand to the BPDE-modified dG residues positioned at the active site of the polymerase. When the 3′-base of the primer strand extends to the base just before the BPDE-modified dG residue (P-1), or to the lesion itself (P), the shapes of the binding curves are quite different from those characterizing the (P-2) complexes and the unmodified (P-2), (P-1), and (P) DNA complexes. The formation of complexes requires higher polymerase concentrations, the shapes of the binding curves are different, and 2:1 dimeric rather than 1:1 monomeric KF^-/DNA complexes are favored. Thus, structural perturbations that hinder the formation of monomeric KF^-/DNA complexes become important only if the BPDE residues are immediately adjacent to the single strand−double strand junction as in (P-1) and (P) complexes.

The NMR solution structures of template−primer complexes with (+)-*trans-anti*-BPDE-N^2-dG lesions with the primer strand extending up to the base before the lesion (analogous to the (P-1) sequence), and up to the lesion (analogous to the (P) sequence), have been reported by Cosman et al. (*6*) and by Feng et al. (*7*), respectively. In both cases, the sequence of the template strand was 5′-d(AAC[G*]CTACCATCC) and that of the template strand was either the 9-mer 5′-d(GGATGGTAG) (*13*) or the 10-mer 5′-d(GGATGGTAGC) (*7*). These NMR sequences are identical to the initial 13 bases, counted from the 5′-end of the template strands of the (P-1) and (P) complexes used in this work, with the two primer strands correspondingly shorter by 10 bases in each case. In the 13-mer/9-mer case (analogous to the (P-1) complex), the hydrophobic BPDE residue is stacked, face-to-face, with the terminal dG residue on the 3′-end of the primer strand; the modified dG residue is thus displaced from its normal position and its glycosidic angle is in the *syn* rather than in the normal *anti* conformation (*6*). In contrast, in the 13-mer/10-mer complex (analogous to the (P) complex), the modified dG residue is base-paired with the terminal dC base on the 3′-end of the 10-mer primer strand, the glycosidic angle is in the *anti* domain, and the BPDE residue is positioned in a partial minor groove (as in full duplexes, *41*), pointing toward the 5′-end of the template strand (*7*). These differences in conformations between the 13-mer/10-mer and 13-mer/9-mer complexes result from subtle interplays between base−base hydrogen bonding and base−carcinogen base stacking interactions (*40*). Both of these conformations constitute, of course, structural perturbations of the single strand−double strand junction in template−primer complexes. An interesting question is whether these conformations at or near the active site of the polymerase are similar or different from these NMR solution structures determined in the absence of enzyme. A recent molecular dynamics simulation with the (+)-*trans-anti*-[BP]-N^2-dG positioned at the active site of pol β indicates that the orientation of the BP residue is similar to the NMR solution structure but that the glycosidic angle is in the normal *anti*, rather than in the *syn*, conformation as in the NMR solution structure; this difference is attributed to interactions between the hydrophobic BP residue and the enzyme (*42*).

The binding of KF^- with template−primer complexes containing (−)-*trans-anti*-BPDE-N^2-dG lesions is only slightly different from those containing (+)-*trans-anti*-BPDE-N^2-dG adducts (Figure 5B,C). NMR solution structures for the 13-mer/9-mer complexes with (−)-*trans-anti*-BPDE-N^2-dG lesions could not be established, but the NMR characteristics of the first three base pairs adjacent to the lesion are partially compromised suggesting that the BPDE residue points into the 3′-direction of the template strand. Despite these differences in the conformational properties of (+)-*trans*- and (−)-*trans-anti*-BPDE-N^2-dG lesions at or near the single strand−double strand junctions in template−primer complexes, the differences in K_{d1} and K_{d2}, if any, are small (Table 1).

Formation of Dimeric Polymerase-Template−Primer Complexes. There is evidence that various polymerase molecules can interact with one another to form dimeric complexes. Using affinity chromatography, Alberts et al. (*43*) found that T4 replicative polymerase molecules may exist as dimers in solution, even in the absence of DNA. Furthermore, T4 DNA polymerase can bind nonspecifically to the single-stranded portion of DNA template−primer complexes (*44*). Moreover, Munn and Alberts (*45*) demonstrated that T4 polymerase

undergoes dimerization at the template−primer junction over a range of polymerase concentrations (27−740 nM), where the first enzyme molecule binds directly to the single strand−double strand junction, and the second one binds to the single-stranded portion of the template. A similar mode of polymerase dimer/DNA template−primer complexes may be operative in the case of our KF^- dimer/DNA complexes.

There may be some physiological reasons underlying the formation of polymerase dimer/DNA complexes. Alberts et al. (*46*) proposed that during DNA replication, at the replication fork, the lagging-strand polymerase is associated with the polymerase molecule on the leading-strand via protein−protein interactions (*45*, *46*). Presumably, the ability of polymerase molecules to associate with one another facilitates these interactions. Indeed, there is more recent evidence demonstrating the presence of and the physical coupling between two polymerase molecules at replication forks. The results of Kim et al. (*47*) and Marians et al. (*48*) suggest that the DNA polymerase III holoenzyme from *E. coli* is a dimer with two catalytic cores held together by the τ subunit. Analysis of the T7 replicative system is also consistent with the presence of two polymerase molecules at the replication fork (*49*−*51*).

Site-Dependent Primer Extension Catalyzed by KF^-. DNA synthesis catalyzed by KF *exo*$^-$ (*52*) or T7 polymerase (*53*) is not significantly influenced by bulky lesions derived from the binding of 2-acetylaminofluorene (AAF) to the C-8 position of dG, as long as dNTP incorporation occurs at template nucleotide positions on the 3′-side of the lesions, but is strongly compromised opposite, or on the 5′-side, of the lesion. The AAF-C8-dG lesions adversely affect the relative primer extension frequency (by factors of 10^3−10^6) catalyzed by KF^- opposite nucleotide positions up to 5 bases on the 5′-side of the lesions on the template strand (*52*). Analogous effects are observed with (+)-*trans*-*anti*-[BP]-N^2-dG lesions in the sequence contexts depicted in Scheme 2 (*21*). The Klenow fragment binds almost normally to BPDE-modified template−primer DNA when there is at least one base on the template strand between the template−primer junction and the [BP]-modified dG residue (Table 1). In the case of such (P-2) complexes, the efficiencies of dGTP insertion opposite the base flanking [dG*] on the 3′-side is decreased by factors of 30−60 relative to unmodified DNA; however, dCTP insertion catalyzed by KF^- is decreased by factors of the order of $\sim 10^5$ opposite [dG*] in the case of the (P-1) complex, and $\sim 10^4$ in the case of single dGTP insertion opposite the dC flanking [dG*] on the 5′-side (P complex).

In summary, the effects of the enzyme/template−primer binding constants on the values of the site-specific steady-state Michaelis−Menten parameter V_{max}, in the vicinity of the lesion site, may not be negligible. In addition, the effects of polymerase concentration and the length of the template strand overhang on the 5′-side of the lesions on polymerase binding and primer extension kinetics should be evaluated as well. These are subjects of further detailed investigations in our laboratory.

SUPPORTING INFORMATION AVAILABLE

Evaluation of dissociation constants K_{d1} and K_{d2} off the Klenow fragment/template−primer complexes and the validity of the mechanism of KF^-/DNA template−primer complex formation. This material is available free of charge via the Internet at http://pubs.acs.org.

REFERENCES

1. Shibutani, S., Margulis, L. A., Geacintov, N. E., and Grollman, A. P. (1993) *Biochemistry 32*, 7531−7541.
2. Shibutani, S., Suzuki, N., Grollman, A. P. (1998) *Biochemistry 37*, 12034−41.
3. Shibutani, S., and Grollman, A. P. (1993) *J. Biol. Chem. 268*, 11703−11710.
4. Singer, B., and Essigman, J. M. (1991) *Carcinogenesis 12*, 949−955.
5. Dzantiev, L., and Romano, L. J. (1999) *J. Biol. Chem. 274*, 3279−3284.
6. Cosman, M., Hingerty, B. E., Geacintov, N. E., Broyde, S., Patel, D. J. (1995) *Biochemistry 34*, 15334−15350.
7. Feng, B., Gorin, A., Hingerty, B. E., Geacintov, N. E., Broyde, S., and Patel, D. J. (1997) *Biochemistry 36*, 13769−13779.
8. Joyce, C. M., Ollis, D. L., Huan, J., Steitz, T. A., Konigsberg, W. H., Grindley N. D. F. (1986) in *Protein Structure, Folding and Design*, pp 197−205, Alan R. Liss, New York.
9. Kolocheva, T. I., Nevinsky, G. A., Volchkova, V. A., Levina, A. S., Khomov, V. V., Lavrik, O. I. (1989) *FEBS Lett. 248*, 97−100.
10. Nevinsky, G. A., Veniaminova, A. G., Levina, A. S., Podust, V. N., Lavrik, O. I., Holler, E. (1990) *Biochemistry 29*, 1200−1207.
11. Harvey, R. G. (1991) *Polycyclic Aromatic Hydrocarbons: Chemistry and Carcinogenicity*, Cambridge University Press, Cambridge, U.K.
12. Meehan, T., and Straub, K. (1979) *Nature* 277, 410−412.
13. Cheng, S. C., Hilton, B. D., Roman, J., M., and Dipple, A. (1989) *Chem. Res. Toxicol. 2*, 334−340.
14. Hruszkewycz, A. M., Canella, K. A., Peltonen, K., Kotrappa, L., and Dipple, A. (1992) *Carcinogenesis 13*, 2347−2352.
15. Hanrahan, C. J., Bacolod, M. D., Vyas, R. R., Liu, T., Geacintov, N. E., Loechler, E. L., and Basu, A. K. (1997) *Chem. Res. Toxicol. 10*, 369−77.
16. Jelynsky, S. A., Liu, T., Geacintov, N. E., and Loechler, E. L. (1995) *Biochemistry 34*, 13545−13553.
17. Moriya, M., Spiegel, S., Fernandes, A., Amin, S., Liu, T., Geacintov, N. E., and Grollman, A. P. (1996) *Biochemistry 31*, 16646−16651.
18. Fernandes, A., Liu, T., Amin, S., Geacintov, N. E., Grollman, A. P., and Moriya, M. (1998) *Biochemistry 37*, 10164−10172.
19. Page, J. E., Zajc, B., Oh-hara, T., Lakshman, M. K., Sayer, J. M., Jerina, D. M., and Dipple, A. (1998) *Biochemistry 37*, 9127−9137.
20. Denissenko, M. F., Pao, A., Tang, M., Pfeifer, G. P. (1996) *Science 274*, 430−432.
21. Li, B. (1995) Ph.D. Dissertation, New York University.
22. Beese, L. S., Derbyshire, V., Steitz, T. A. (1993) *Science 260*, 352−355.
23. Beese, L. S., Friedman, J. M., and Steitz, T. A. (1993) *Biochemistry 32*, 14095−14101.
24. Johnson, K. A., and Steitz, T. A. (1994) *Annu. Rev. Biochem. 63*, 777−822.
25. Derbyshire, V., Freemont, P. S., Sanderson, M. R., Beese, L., Friedman, J. M., Joyce, C. M., and Steitz, T. A. (1988) *Science 240*, 199−201.
26. Eger, B. T., Kuchta, R. D., Carroll, S. S., Benkovic, P. A., Dahlberg, M. E., Joyce, C. M., and Benkovic, S. J. (1991) *Biochemistry 30*, 1441−1448.
27. Johnson, K. A. (1993) *Annu. Rev. Biochem. 62*, 685−713.
28. McLaughlin, L. W., and Piel, N. (1984) in *Oligonucleotide Synthesis: a Practical Approach* (Gait, M. J., Ed.) pp 117−133, IRL Press, Oxford, Washington, DC.
29. Cosman, M., Ibanez, V., Geacintov, N. E., Harvey, R. G. (1990) *Carcinogenesis 11*, 1667−72.
30. Geacintov, N. E., Cosman, M., Mao, B., Alfano A., Ibanez, V., and Harvey, R. G. (1991) *Carcinogenesis 12*, 2099−2108.

31. Xu, R., Mao, B., Xu, J., Li, B., Birke, S., Swenberg, C. E., Geacintov, N. E. (1995) *Nucleic Acids Res. 23*, 2314−2319.
32. Liu, T., Xu, J., Li, B., Xu, R., Yang, C., Moryia, M., and Geacintov, N. E. (1995) *Chem. Res. Toxicol. 9*, 255−261.
33. Suh, M., Ariese, F., Small, G. J., Jankowiak, R., Liu, T. M., Geacintov, N. E. (1995) *Biophys. Chem. 56*, 281−96.
34. Tsao, H., Mao, B., Zhuang, P., Xu, R., Amin, S., Geacintov, N. E. (1998) *Biochemistry 37*, 4993−5000.
35. Astatke, M., Grindley, N. D. F., and Joyce, C. M. (1995) *J. Biol. Chem. 270*, 1945−1954.
36. Ferguson, K. A. (1964) *Metabolism 13*, 985−1002.
37. Kuchta, R. D., Mizrahi, V., Bencovic, P. A., Johnson, K. A., and Benkovic, S. J. (1987) *Biochemistry 26*, 8410−8417
38. Bryant, F. R., Johnson, K. A., and Benkovic, S. J. (1983) *Biochemistry 22*, 3537−3546.
39. Patel, D. J., Mao, B., Gu Z., Hingerty, B. E., Gorin, A., Basu, A. K., and Broyde, S. (1998) *Chem. Res. Toxicol. 11*, 391−407.
40. Geacintov, N. E., Cosman, M., Hingerty, B. E., Amin, S., Broyde, S., Patel, D. J. (1997) *Chem. Res. Toxicol. 10*, 111−146.
41. Cosman, M., de los Santos, C., Fiala, R., Hingerty, B. E., Singth, S. B., Ibanez, V., Margulis, L. A., Live, D., Geacintov, N. E., Broyde, S., and Patel, D. J. (1992) *Proc. Natl. Acad. Sci. U.S.A. 89*, 1914−1918.
42. Singh, S. B., Beard, W. A., Hingerty, B. E., Wilson, S. H., and Broyde, S. (1998) *Biochemistry 37*, 878−884.
43. Alberts, B. M., Barry, J., Bedinger, P., Formosa, T., Jongeneel, C. V., and Kreuzre, K. N. (1983) *Cold Spring Harbor Symp. Quantum Biol. 47*, 655−668.
44. Mace, D. C., and Alberts, B. M., (1984) *J. Mol. Biol. 177*, 295−311.
45. Munn, M. M., and Alberts, B. M. (1991) *J. Biol. Chem. 266*, 20034−20044.
46. Alberts, B. M., Morris, C., Mace, D., Sinha, N., Bittner, M., and Morgan, L. (1975) in *DNA Synthesis and Its Regulation* (Goulian, M., and Hanawalt, P., Eds.) pp 241−269, W. A. Benhamin, Inc., Menlo Park, CA.
47. Kim, S., Dallman, H. G., McHenry, C. S., and Marians, K. J. (1996) *J. Biol. Chem. 271*, 21406−21412.
48. Marians, K. J., Hiasa H., Kim, D. R., and McHenry, C. S. (1998) *J. Biol. Chem. 273*, 2452−2457.
49. Lee, J., Chastain, P. D., II, Kusakabe, T., Griffith, J. D., Richardson, C. C. (1998) *Mol. Cell 1*, 1001−1010.
50. Park, K., Debyser, Z., Tabor, S., Richardson, C. C., and Griffith, J. D. (1998) *J. Biol. Chem. 273*, 5260−5270.
51. Debyser, Z., Tabor, S., and Richardson, C. C. (1994) *Cell 77*, 157−166.
52. Miller, H., and Grollman, A. P. (1997) *Biochemistry 36*, 15336−15342.
53. Lindsley, J. E., and Fuchs, R. P. P. (1994) *Biochemistry, 33*, 764−772.

BI990614K